Physics of the Solid State, Vol. 46, No. 6, 2004, pp. 1088–1094. Translated from Fizika Tverdogo Tela, Vol. 46, No. 6, 2004, pp. 1058–1064.

MAGNETISM AND FERROELECTRICITY

Mössbauer Effect Study in $Fe_{1-x}V_xBO_3$ Solid Solutions

O. A. Bayukov*, M. M. Abd-Elmeguid, N. B. Ivanova***, N. V. Kazak*, S. G. Ovchinnikov*, and V. V. Rudenko***

**Kirensky Institute of Physics, Siberian Division, Russian Academy of Sciences, Akademgorodok, Krasnoyarsk, 660036 Russia*

***Physikalisches Institut, Universität zu Köln, Köln, 50937 Germany*

****Krasnoyarsk State Technical University, Krasnoyarsk, 660074 Russia*

Received September 16, 2003; in final form, November 13, 2003

Abstract—The Mössbauer effect in the $Fe_{1-x}V_xBO_3$ solid solutions has been measured at 130 and 300 K. The $Fe_{0.05}V_{0.95}BO_3$ composition was studied in the interval 4.2–300 K. The experimental data obtained are described in terms of the model of a dilute magnetic insulator in which atoms of the first coordination sphere provide a major contribution to the hyperfine field at iron nucleus sites. It was found that, at low temperatures, the field H_{hf} is generated primarily by the iron ion itself and depends only weakly on substitution. The hyperfine interaction parameters in the discrete configuration series 6Fe, 5Fe1V, 4Fe2V, 3Fe3V, and 2Fe4V were determined. The magnitude of the isomer shift suggests that iron in the crystal resides in the trivalent state. © *2004 MAIK "Nauka/Interperiodica".*

1. INTRODUCTION

Transition metal borates with the chemical formula MBO_3 crystallize in the calcite structure [space group $R\bar{3}c(D_{3d}^6)$]. Strong electronic correlations offer the possibility of observing the rich variety of magnetic structures and electronic properties in this series of compounds governed by the presence of one or another transition metal M^{3+} = Fe, V, Cr, or Ti. $FeBO_3$ has been a subject of intense interest since the time it was first prepared [1]; studies were made on its optical and magnetooptical properties [2–6], crystal structure [7, 8], magnetic properties [9–11], and NMR [12, 13] and Mössbauer [14, 15] spectra. The $FeBO_3$ iron borate is transparent in the visible region, and its magnetic ordering temperature is above room temperature, T_N = 348 K. Unfortunately, experimental information on other representatives of this class of borates is scarce. The isostructural compounds VBO_3, $CrBO_3$, and $TiBO_3$ were first synthesized in 1964 [16]. VBO_3 is known to be a ferromagnetic semiconductor with T_C = 32 K, and $CrBO_3$ is a low-temperature antiferromagnet with T_N = 15 K and an insulator [17]. $TiBO_3$ was reported to be a weak ferromagnet (T_N = 25 K) [18]. There are publications on studies of hyperfine interaction in iron borate–based solid solutions $Fe_{1-x}M_xBO_3$, where the ions M = Al, Ga, and Cr act as substituting ions [19–21].

A coordinated investigation of the magnetic, electrical, and optical properties of $Fe_{1-x}V_xBO_3$ solid solutions was performed earlier in [22]. This communication reports on a measurement of the Mössbauer effect in iron-containing samples of $Fe_{1-x}V_xBO_3$.

2. SAMPLES AND EXPERIMENTAL TECHNIQUES

The $Fe_{1-x}V_xBO_3$ single crystals under study were grown by spontaneous crystallization from a melt solution [22]. The crystals were hexagonal platelets up to 4×4 mm in size and about 0.1 mm thick. The concentration x quoted in [22] was derived from the content of components in the charge (x_{ch}). The exact amounts of the elements were determined by EDAX ZAF quantification. The values of x thus obtained are listed in Table 1 together with the earlier x_{ch} figures.

Mössbauer measurements were performed on powdered samples of the $Fe_{1-x}V_xBO_3$ single crystals. The isomer shift δ was determined relative to metallic (α-Fe) iron.

The experiments on the $Fe_{1-x}V_xBO_3$ samples were carried out at 130 and 300 K with a Co^{57}(Cr) source. The optimum sample thickness was calculated with due account of the iron content and the absorption factor and was found to be 5–10 mg Fe/cm^2. The model spectra were least squares fitted to experimental data under the assumption that the spectral lines have Lorentzian shape. We took as an additional fitting parameter the

Table 1. Vanadium concentration in $Fe_{1-x}V_xBO_3$ solid solutions

x_{ch}	0.25	0.5	0.6	0.75	0.95
x	0.02	0.13	0.18	0.3	0.95

Note: x_{ch} was derived from the content of components in the charge, and x, from energy-dispersive analysis of x-rays (EDAX ZAF quantification).

broadening of the outer sextet lines with respect to the inner lines (Γ_{16}/Γ_{34}), which is proportional to the hyperfine field at the nucleus site. Processing of the experimental spectra revealed the presence of an impurity phase, Fe_3BO_6, in the solid solutions, which should be assigned to the crystallization temperatures of these compounds being very similar and was described earlier in [21].

The spectra of the $Fe_{0.05}V_{0.95}BO_3$ crystal in the range of 4.2 to 300 K were measured with a Co^{57}(Rh) source of an initial activity of 25 mCi (925 MBq). The measurements were performed in the transmission geometry. The source was placed inside a ^{4}He cryostat close to the sample. The maximum source velocity was

$$V_{\max} = CU_{\text{eff}},$$

where U_{eff} is the effective amplitude of the sine signal and C is the calibration factor, equal to 0.041326 mm/s mV. The measurements were performed on polycrystalline samples containing 1 mg Fe/cm^2 that were mixed thoroughly with Al_2O_3.

3. EXPERIMENTAL RESULTS

Figure 1 shows Mössbauer spectra of $Fe_{1-x}V_xBO_3$ solid solutions obtained at room temperature. The $FeBO_3$ spectrum is a well-resolved sextet (Fig. 1, *a*). The hyperfine interaction parameters are in agreement with the data from [14]. The spectral line intensities are in the ratio 3 : 2 : 1 : 1 : 2 : 3.

Because of the compositional disorder characteristic of solid solutions, impurity atoms can be considered to be distributed randomly in the matrix. Thus, all the cation states are equivalent and can be occupied by iron and vanadium atoms in random fashion. Because the exchange interactions have short-range character, we analyze experimental spectra in the nearest neighbor approximation. The central iron atom has n atoms of vanadium and $(6 - n)$ atoms of iron in its nearest environment. The probability of finding such atomic configurations in a crystal is described by the well-known binomial distribution

$$P_6(n) = \frac{6!}{n!(6-n)!}(1-x)^n x^{6-n},$$

where x is the vanadium concentration. The local molecular field theory was applied to interpret complex Mössbauer spectra of mixed oxide systems in [23].

Following this assumption, the spectrum of the $Fe_{0.98}V_{0.02}BO_3$ crystal (Fig. 1, *b*) can be unfolded into two sextets with occupations of 76 and 24%. The former sextet relates to the nearest iron environment consisting of six iron atoms (6Fe), and the latter sextet, to the configuration in which there is one vanadium atom among the nearest neighbors (5Fe1V). The probability distributions of hyperfine fields at the iron nucleus sites and the calculated hyperfine interaction

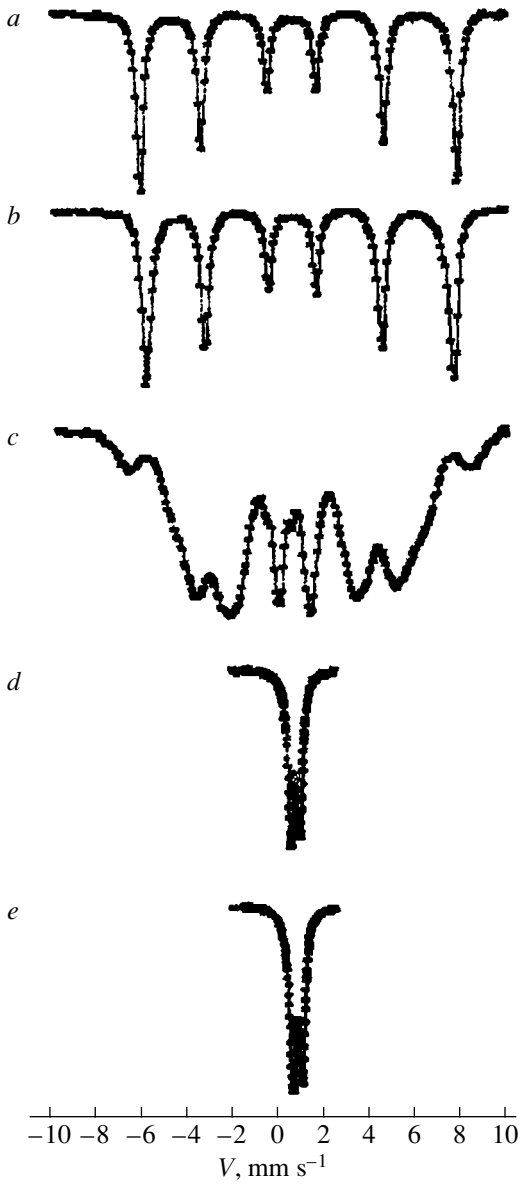

Fig. 1. Mössbauer spectra of (*a*) $FeBO_3$, (*b*) $Fe_{0.98}V_{0.02}BO_3$, (*c*) $Fe_{0.87}V_{0.13}BO_3$, (*d*) $Fe_{0.82}V_{0.18}BO_3$, and (*e*) $Fe_{0.7}V_{0.3}BO_3$ obtained at 300 K.

parameters in the solid solutions are displayed in Fig. 2 and listed in Table 2. It is assumed that the hyperfine field in insulators is well described in the nearest neighbor approximation; therefore, the fields of the 6Fe, 5Fe1V, 4Fe2V, etc., configurations are discrete and well resolved and the 6Fe configuration in a substituted crystal has the same hyperfine field as in an unsubstituted one. In our case, while the 5Fe1V configuration (H_{hf} = 323 kOe) differs noticeably from the 6Fe configuration (H_{hf} = 335 kOe), the field of 335 kOe is substantially smaller than H_{hf} = 345 kOe in the unsubstituted borate $FeBO_3$. Quite probably, the hyperfine field at

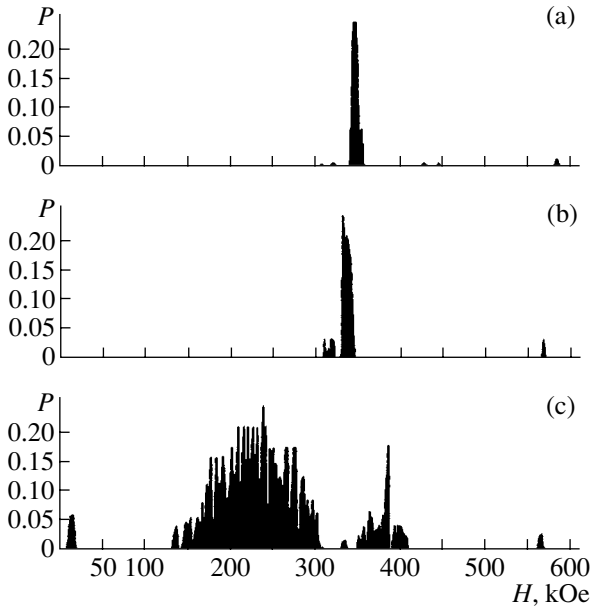

Fig. 2. Hyperfine field probability distribution for iron nuclei at 300 K obtained for (a) $FeBO_3$, (b) $Fe_{0.98}V_{0.02}BO_3$, and (c) $Fe_{0.87}V_{0.13}BO_3$.

iron nucleus sites in $FeBO_3$ is contributed to markedly by next-to-nearest neighbors.

The spectrum of the $Fe_{0.87}V_{0.13}BO_3$ has a complex shape (Fig. 1, *c*). The distribution of the hyperfine field probabilities allows us to isolate three regions (Fig. 2c). The region of 350–400 kOe corresponds to fields higher than the field in $FeBO_3$ but lower than that in Fe_3BO_6, H_{hf} = 521 kOe [24]. This region can be assigned to the vanadium-substituted Fe_3BO_6 phase. The broad region of 150–300 kOe can be identified with the $Fe_{1-x}V_xBO_3$ crystal. The width of the hyperfine field distribution for the $Fe_{1-x}V_xBO_3$ crystal is larger than that for the substituted Fe_3BO_6 phase. This may be explained by the fact that the iron in Fe_3BO_6 has a larger number of magnetic bonds (6 for the 8*d* and 8 for 4*c* sites, symmetry group P_{nma}) [25] compared to $FeBO_3$ (6 bonds) and that the number of magnetic bonds is a factor that stabilizes the hyperfine field. Moreover, the Néel temperature of $FeBO_3$ (348 K) is substantially lower than that of Fe_3BO_6 (508 K) [26]. Note also that the degree of vanadium substitution for the $FeBO_3$ crystal is larger than that for Fe_3BO_6. The hyperfine field probability distribution in the 150- to 300-K region is almost symmetrical, with a slight deviation toward higher fields. The experimental spectrum is fitted well by a set of sextets, whose parameters are listed in Table 2. In accordance with the binomial distribution, their assignment is specified by the number of Fe and V neighbors. The weak peak in the hyperfine field probability distribution in the low field region is due to a paramagnetic doublet, which probably belongs

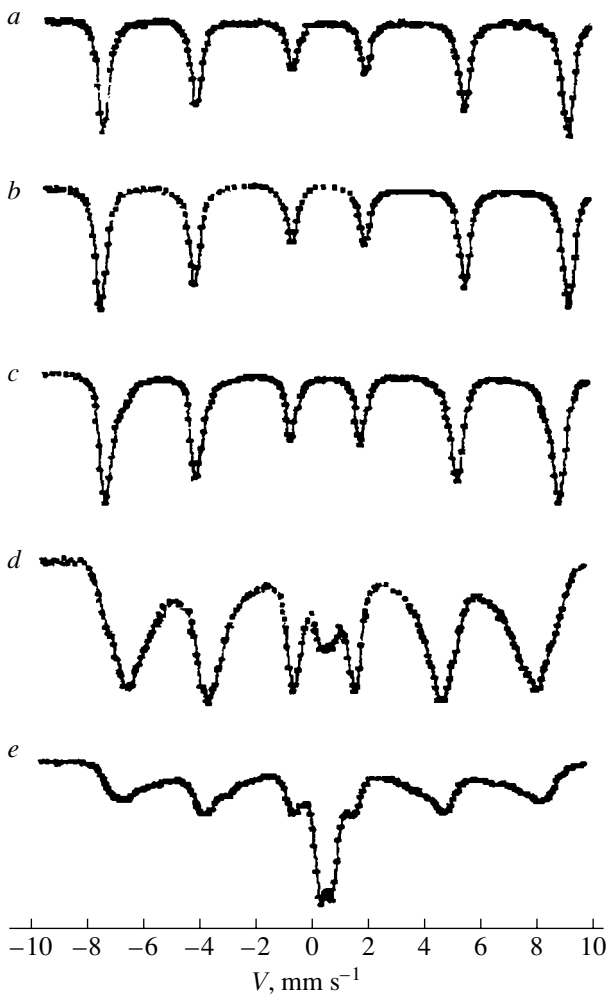

Fig. 3. Mössbauer spectra of (*a*) $FeBO_3$, (*b*) $Fe_{0.98}V_{0.02}BO_3$, (*c*) $Fe_{0.87}V_{0.13}BO_3$, (*d*) $Fe_{0.82}V_{0.18}BO_3$, and (*e*) $Fe_{0.7}V_{0.3}BO_3$ obtained at T = 130 K.

to superparamagnetic regions in $Fe_{1-x}V_xBO_3$ or to the substituted Fe_3BO_6.

The room-temperature spectra of the $Fe_{1-x}V_xBO_3$ solid solutions with vanadium concentrations x = 0.18, 0.3, and 0.95 represent quadrupole doublets with asymmetry in the intensities of the 3/2 ⟶ 1/2 and 1/2 ⟶ 1/2 nuclear transitions. This could be assigned to the crystallite *c* axes being oriented preferentially parallel to the γ-ray direction; however, we study here powder samples and the observed asymmetry is actually a manifestation of the Gol'danskii–Karyagin effect [27]. This effect is small for monoclinic lattices and, hence, the asymmetry is due to the rhombohedral lattice of the $Fe_{1-x}V_xBO_3$ crystal. We may thus conclude that each doublet can be unfolded into two doublets, symmetric and asymmetric.

Figures 3 and 4 display the Mössbauer spectra and the distribution functions of the hyperfine field probability at iron nucleus sites, respectively, obtained for the

Table 2. Hyperfine interaction parameters in $Fe_{1-x}V_xBO_3$ solid solutions obtained at 300 K

Compound	δ	H_{hf}	ΔE_Q	Γ_{34}	Γ_{16}/Γ_{34}	S	Assignment
$FeBO_3$	0.40	345	0.38	0.29	1	1	"$FeBO_3$"
$Fe_{0.98}V_{0.02}BO_3$	0.40	335	0.39	0.30	1.04	0.76	6Fe
	0.39	323	0.36	0.30	1.58	0.24	5Fe1V
$Fe_{0.87}V_{0.13}BO_3$	0.39	278	0.41	0.43	1.72	0.20	6Fe
	0.40	251	0.41	0.43	1	0.11	5Fe1V
	0.39	231	0.38	0.41	1	0.14	4Fe2V
	0.39	212	0.36	0.38	1	0.12	3Fe3V
	0.39	189	0.41	0.30	1.91	0.13	2Fe4V
	0.38	159	0.30	0.53	1.58	0.13	1Fe5V
	0.44			1.31		0.06	–
	0.36	375	0.54	0.20	5.26	0.11	"Fe_3BO_6"
$Fe_{0.82}V_{0.18}BO_3$	0.42		0.40	0.28		0.70	"$FeBO_3$" (GKE = 1.1)
	0.38		0.47	0.32		0.30	"Fe_3BO_6"
$Fe_{0.7}V_{0.3}BO_3$	0.41		0.42	0.32		0.71	"$FeBO_3$" (GKE = 1.09)
	0.40		0.45	0.30		0.29	"Fe_3BO_6"
$Fe_{0.05}V_{0.95}BO_3$	0.42		0.43	0.17		0.43	"$FeBO_3$" (GKE = 1.67)
	0.39		0.48	0.39		0.57	

Note: δ is the isomer chemical shift relative to metallic iron (αFe), ±0.02 mm/s; H_{hf} is the hyperfine field at an iron nucleus site, ±5 kOe; ΔE_Q is the quadrupole splitting, ±0.04 mm/s; Γ_{34} is the FWHM of inner sextet lines, ±0.02 mm/s; Γ_{16}/Γ_{34} is the ratio of the outer to inner sextet line widths, ±0.04 mm/s; S is the fractional site occupation, ±0.05; and GKE stands for the Gol'danskii–Karyagin effect.

$Fe_{1-x}V_xBO_3$ solid solutions at 130 K. The temperature dependences of the hyperfine field for $FeBO_3$ and Fe_3BO_6 are known to cross in the temperature region close to 240 K, and the resolution of the sextets becomes poorer as the temperature is lowered [21]. The hyperfine field probability distribution function does not permit identification of the individual iron positions 6Fe and 5Fe1V (Fig. 4b) for the $Fe_{0.98}V_{0.02}BO_3$ crystal. Deconvolution into two sextets makes it possible to evaluate the probable occupations of these configurations. For the same reason, one cannot reliably determine the occupations of the inequivalent positions in the $Fe_{0.87}V_{0.13}BO_3$ composition (Fig. 4c).

The Mössbauer spectra of $Fe_{0.82}V_{0.18}BO_3$ and $Fe_{0.7}V_{0.3}BO_3$ samples measured at 130 K are superpositions of several sextets and of a paramagnetic doublet (Figs. 3d, 3e). This complexity of the hyperfine interaction pattern can originate from the nonuniform magnetic state occurring in these crystals. Local deviations from stoichiometry are capable of affecting magnetic order in the sample. The temperature dependence of the magnetization of these solid solutions follows a nontrivial pattern and exhibits two magnetic transitions in the temperature range from 30 to 200 K [22]. The broad hyperfine field distribution observed in the $Fe_{0.82}V_{0.18}BO_3$ and $Fe_{0.7}V_{0.3}BO_3$ crystals (Figs. 4d, 4e) allows isolation of a discrete set of the 6Fe, 5Fe1V, 4Fe2V, 3Fe3V, and 2Fe4V configurations, whose hyperfine parameters are listed in Table 3. The binomial distribution passes through a maximum at the 5Fe1V configuration (17%) for the $x = 0.18$ composition and at the 6Fe configuration (15%) for the composition with $x = 0.3$. The isomer shift is the same for all positions to within experimental error. The spectra obtained suggest the existence of a vanadium-diluted superparamagnetic phase of Fe_3BO_6.

The $Fe_{0.05}V_{0.95}BO_3$ solid solution remains paramagnetic down to 130 K. To gain deeper insight into the hyperfine interactions in this crystal, we performed Mössbauer studies at temperatures spanning the range from 4.2 to 300 K. The results of calculations and measurements are listed in Table 4 and presented in graphical form in Fig. 5. The spectrum of the $Fe_{0.05}V_{0.95}BO_3$ composition measured at 4.2 K is a sextet with an admixture of the paramagnetic phase, which adds up to not over 10% of the magnetically ordered phase (Fig. 5a). The relative sextet line intensities are close to 3 : 2 : 1 : 1 : 2 : 3. The hyperfine field H_{hf} at iron nucleus sites in this sample is 507 kOe, which is 8.6% lower than that in the unsubstituted $FeBO_3$ crystal (555 kOe) measured at the same temperature [14]. The nearest neighbor contribution to the effective hyperfine field at iron nucleus sites in $FeBO_3$ is approximately 10% of the ion-core spin polarization. The lower effective field H_{hf} in $Fe_{0.05}V_{0.95}BO_3$ compared to that in $FeBO_3$ can be assigned to the perturbation introduced by vanadium impurity atoms.

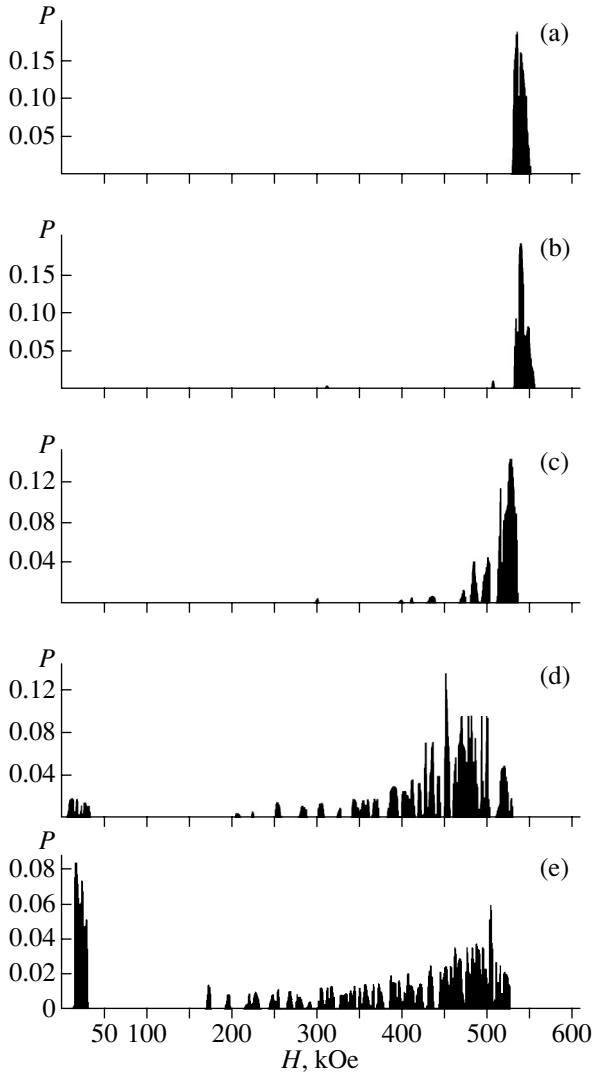

Fig. 4. Hyperfine field probability distribution for iron nuclei obtained at T = 130 K for (a) $FeBO_3$, (b) $Fe_{0.98}V_{0.02}BO_3$, (c) $Fe_{0.87}V_{0.13}BO_3$, (d) $Fe_{0.82}V_{0.18}BO_3$, and (e) $Fe_{0.7}V_{0.3}BO_3$.

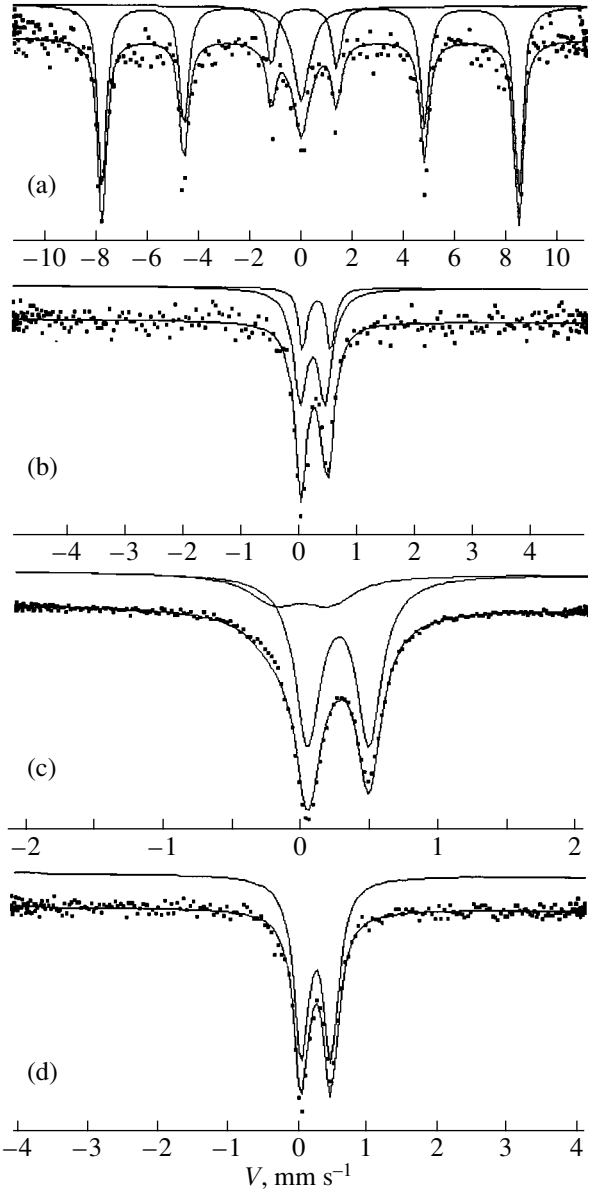

Fig. 5. Mössbauer spectra of a $Fe_{0.05}V_{0.95}BO_3$ crystal obtained at temperatures of (a) 4.2, (b) 70, (c) 130, and (d) 300 K.

The Mössbauer spectra of the sample obtained at 70 and 130 K are asymmetric doublets characteristic of the paramagnetic state (Figs. 5b, 5c). Each spectrum can be unfolded into doublets relating to different atomic configurations. According to the binomial distribution, for a vanadium concentration x = 0.95, the probable occupations of the 6V and 1Fe5V configurations acquire maximum values of 76 and 25%, respectively. The two doublets characterizing these configurations are identified in the figures by solid lines. The isomer shifts for these configurations are independent of temperature and are δ = 0.23 mm/s for iron in the 6V position and δ = 0.29 mm/s for the 1Fe5V environment. These configurations have a constant quadrupole splitting (Table 4). Unfortunately, the poor resolution of the $Fe_{0.05}V_{0.95}BO_3$ spectrum does not allow isolation and identification of the inequivalent iron positions at room temperature (Fig. 5d).

4. DISCUSSION OF THE RESULTS

Thus, deconvolution of solid-solution spectra into constituent spectra of the components of these solutions, which was made under the assumption of a random impurity distribution and of additivity of the contributions due to impurity atoms to H_{hf} and δ and with due account of the influence of atoms in the first coordination sphere, has permitted us to evaluate the hyperfine parameters for the 6Fe, 5Fe1V, 4Fe2V, 3Fe3V, and

Table 3. Hyperfine interaction parameters for $Fe_{1-x}V_xBO_3$ solid solutions obtained at 130 K

Compound	δ	H_{hf}	ΔE_Q	Γ_{34}	Γ_{16}/Γ_{34}	S	Assignment
$FeBO_3$	0.50	540	0.46	0.47	1	1	"$FeBO_3$"
$Fe_{0.98}V_{0.02}BO_3$	0.50	539	0.37	0.44	1	0.87	6Fe
	0.49	528	0.33	0.32	1	0.13	5Fe1V
$Fe_{0.87}V_{0.13}BO_3$	0.50	524	0.39	0.46	1.05	0.76	"$FeBO_3$"
	0.50	491	0.44	0.51	1.19	0.19	"$FeBO_3$"
	0.50	425	0.07	0.87	1.01	0.05	"Fe_3BO_6"
$Fe_{0.82}V_{0.18}BO_3$	0.51	514	0.41	0.28	2.54	0.10	6Fe
	0.51	484	0.44	0.50	1.15	0.17	5Fe1V
	0.51	462	0.45	0.44	1.13	0.14	4Fe2V
	0.51	436	0.43	0.48	1	0.11	3Fe3V
	0.52	403	0.54	0.53	1.11	0.08	2Fe1V
	0.52	351	0.41	0.36	12.3	0.30	"Fe_3BO_6"
	0.46			1.31		0.1	"Fe_3BO_6"
$Fe_{0.7}V_{0.3}BO_3$	0.51	501	0.41	0.41	1.49	0.15	6Fe
	0.50	471	0.49	0.45	1.40	0.14	5Fe1V
	0.49	430	0.49	0.57	1.94	0.12	4Fe2V
	0.50	374	0.45	0.56	1.06	0.13	3Fe3V
	0.49	273	0.30	1.77	1.06	0.22	"Fe_3BO_6"
	0.49		0.43	0.51		0.23	"Fe_3BO_6"
$Fe_{0.05}V_{0.95}BO_3$	0.50		0.44	0.48		1	"$FeBO_3$"

Note: δ, ±0.02 mm/s; H_{hf}, ±5 kOe; ΔE_Q, ±0.04 mm/s; Γ_{34}, ±0.02 mm/s; Γ_{16}/Γ_{34}, ±0.04 mm/s; and S, ±0.05.

Table 4. Hyperfine interaction parameters for a $Fe_{0.05}V_{0.95}BO_3$ crystal obtained at different temperatures

T, K	δ	H_{hf}	ΔE_Q	Γ_{34}	S	Assignment
4.2	0.28 ± 0.005	507.2 ± 0.03	0.22 ± 0.01	0.40 ± 0.02		
70	0.23 ± 0.01		0.42 ± 0.01	0.29 ± 0.023	0.75	6V
	0.29 ± 0.013		0.48 ± 0.016	0.16 ± 0.02	0.25	1Fe5V
130	0.23 ± 0.003		0.42 ± 0.004	0.33 ± 0.007	0.76	6V
	0.29 ± 0.002		0.47 ± 0.003	0.14 ± 0.004	0.24	1Fe5V
300	0.27 ± 0.002		0.43 ± 0.003	0.26 ± 0.005		

Note: δ, ±0.01 mm/s; H_{hf}, ±0.03 kOe; ΔE_Q, ±0.02 mm/s; Γ_{34}, ±0.02 mm/s; and S, ±0.02.

2Fe4V positions in the $Fe_{0.87}V_{0.13}BO_3$ crystal at room temperature and in the $Fe_{0.82}V_{0.18}BO_3$ and $Fe_{0.7}V_{0.3}BO_3$ crystals at a temperature of 130 K. The hyperfine fields at iron nucleus sites decrease monotonically in the series of these configurations in discrete steps of ΔH_{hf} = 20–30 kOe, in full agreement with the usual concepts concerning a dilute magnetic insulator. The chemical isomer shifts for these configurations are the same to within experimental error. The isomer shifts at room temperature, δ = 0.38–0.40 mm/s, and at 130 K, δ = 0.51–0.52 mm/s, indicate that iron in the $Fe_{1-x}V_xBO_3$ system is trivalent. Note that the idea of substitution of an average-sized ion used in [28] to interpret Mössbauer spectra of the $(Fe_{1-x}V_x)_2O_3$ system, according to which low vanadium contents are conducive to the formation of Fe^{2+}–V^{4+} ion pairs, did not find support in our studies. This implies that the electronic state of iron does not depend on substitution by vanadium. The iron ion resides in an octahedral environment, and the electric field gradient at iron nucleus sites is directed parallel to the [111] threefold axis. The quadrupole splitting in the $Fe_{1-x}V_xBO_3$ solid solutions is close in magnitude to ΔE_Q = 0.46 mm/s, the value for the unsubstituted $FeBO_3$ crystal. The small change in the hyperfine field for the $Fe_{0.05}V_{0.95}BO_3$ sample at 4.2 K compared to that in $FeBO_3$ indicates that the H_{hf} field in these crystals is

produced primarily by the iron ion itself and depends only weakly on the environment.

ACKNOWLEDGMENTS

One of the authors (M.M. A.-E.) would like to thank the Deutsche Forschungsgemeinschaft for financial support (SFB 608).

This study was supported by the Russian Foundation for Basic Research (project no. 03-02-16286) and the federal program "Integration" (project no. B0017).

REFERENCES

1. I. Bernal, C. W. Struck, and J. G. White, Acta Crystallogr. **16**, 849 (1963).
2. J. Haisma, H. J. Prins, and K. L. L. van Mierlo, J. Phys. D: Appl. Phys. **7**, 162 (1974).
3. B. Andlauer, J. Schneider, and W. Wettling, Appl. Phys. **10**, 189 (1976).
4. R. Wolfe, A. J. Kurtzig, and R. C. LeCraw, J. Appl. Phys. **41**, 1218 (1970).
5. I. S. Édel'man and A. V. Malakhovskiĭ, Opt. Spektrosk. **35**, 959 (1973).
6. A. J. Kurtzig, R. Wolfe, R. C. LeCraw, and J. W. Nielsen, Appl. Phys. Lett. **14**, 350 (1969).
7. R. Diehl, Solid State Commun. **17**, 743 (1975).
8. M. Pernet, D. Elmaleh, and J.-C. Joubert, Solid State Commun. **8**, 1583 (1970).
9. J. C. Joubert, T. Shirk, W. B. White, and R. Roy, Mater. Res. Bull. **3**, 671 (1968).
10. A. S. Kamzin, B. Shtahl, R. Gellert, M. Muller, E. Kankeleit, and D. B. Vcherashniĭ, Pis'ma Zh. Éksp. Teor. Fiz. **71**, 197 (2000) [JETP Lett. **71**, 134 (2000)].
11. A. M. Kodomtseva, R. Z. Levitin, Yu. F. Popov, V. N. Seleznev, and V. V. Uskov, Fiz. Tverd. Tela (Leningrad) **14**, 214 (1972) [Sov. Phys. Solid State **14**, 172 (1972)].
12. M. P. Petrov, G. A. Smolenskiĭ, A. P. Paugurt, S. A. Kizhaev, and M. K. Chizhov, Fiz. Tverd. Tela (Leningrad) **14**, 109 (1972) [Sov. Phys. Solid State **14**, 87 (1972)].
13. L. V. Velikov, E. G. Rudashevskiĭ, and V. N. Seleznev, Izv. Akad. Nauk SSSR, Ser. Fiz. **36**, 1531 (1972).
14. M. Eibschutz, L. Pfeiffer, and J. W. Nielsen, J. Appl. Phys. **41**, 1276 (1970).
15. M. Kopcewicz, H. Engelmann, S. Stenger, G. V. Smirnov, U. Gonser, and H. G. Wagner, Appl. Phys. A **44**, 131 (1987).
16. H. Schmid, Acta Crystallogr. **17**, 1080 (1964).
17. T. A. Bither, Carol G. Frederick, T. E. Gier, J. F. Weiher, and H. S. Young, Solid State Commun. **8**, 109 (1970).
18. Xu Ziguang, Matam Mahesh Kumar, and Ye Zuo Guang, in *Proceedings of Annual March Meeting* (Am. Phys. Soc., 2001).
19. De Lacklison, J. Chadwick, and J. L. Page, J. Phys. D: Appl. Phys. **5**, 810 (1972).
20. M. W. Ruckman, R. A. Levy, and R. Chennette, J. Appl. Phys. **53**, 1694 (1982).
21. O. A. Bayukov, V. P. Ikonnikov, M. I. Petrov, V. V. Rudenko, V. N. Seleznev, and V. V. Uskov, Tr. MKM-73b **3**, 313 (1974).
22. N. B. Ivanova, V. V. Rudenko, A. D. Balaev, N. V. Kazak, V. V. Markov, S. G. Ovchinnikov, I. S. Édel'man, A. S. Fedorov, and P. V. Avramov, Zh. Éksp. Teor. Fiz. **121**, 354 (2002) [JETP **94**, 299 (2002)].
23. J. M. D. Coey and G. A. Sawatzky, Phys. Status Solidi B **44**, 673 (1971).
24. A. S. Kamzin and L. A. Grigor'ev, Zh. Éksp. Teor. Fiz. **105**, 377 (1994) [JETP **78**, 200 (1994)].
25. J. G. White, A. Miller, and R. E. Nielsen, Acta Crystallogr. **19**, 1060 (1965).
26. M. Hirano, T. Okuda, T. Tsushima, S. Umemura, K. Kohn, and S. Nakamura, Solid State Commun. **15**, 1129 (1974).
27. V. I. Goldanskii, E. F. Markov, and V. V. Karpov, Phys. Lett. **3**, 344 (1963).
28. G. Shirane, D. E. Cox, and S. L. Ruby, Phys. Rev. **125**, 1158 (1962).

Translated by G. Skrebtsov